8

The Carbon Isotope Record and Earth Surface Oxygenation

Thomas A. Laakso and Daniel P. Schrag

ABSTRACT

Carbon isotopes in ancient marine carbonates have long been thought to record organic carbon burial rates (Knoll et al., 1986). However, the carbon isotopic composition ($\delta^{13}C$) of carbonates has been relatively stable for the last three billion years, suggesting limited variability in the oxygen production associated with organic carbon burial. This suggests that oxygen production far outpaced oxygen consumption during oxygen-poor portions of Earth history, given that the rate of oxidative reactions are themselves sensitive to atmospheric oxygen levels. However, an unbalanced oxygen budget is at odds with overwhelming evidence for billions of years of low-oxygen conditions during the Precambrian and early Paleozoic. We propose that the $\delta^{13}C$ of carbonates is in fact not a reliable record of oxygen production. Rather, it is controlled by oxygen-sensitive precipitation of isotopically depleted authigenic carbonates, a negative feedback that regulates the $\delta^{13}C$ of platform carbonates and partially decouples that record from the rate of organic carbon burial on geologic timescales.

8.1. INTRODUCTION

The reduction and subsequent burial of carbon by photosynthetic organisms is the only significant source of free O_2 to the atmosphere. Redox proxies suggest that oxygen concentrations have varied by many orders of magnitude over Earth history, increasing by large margins both at 2.4 Ga, and again in the late Neoproterozoic and early Paleozoic (Lyons et al., 2014). The exact timing of this latter event, and its causal connections to the origin and diversification of multicellularity and motility, remain controversial (Sperling et al., 2015). This problem is exacerbated by the lack of a direct record of oxygen levels, which must be inferred from proxies that are at best weakly quantitative. The record of organic carbon burial and oxygen generation recorded in the rich carbon isotope record of calcium carbonate has been an important tool in untangling these problems (Des Marais et al., 1992).

During photosynthetic fixation of carbon, a large isotope fractionation is imparted to the organic carbon, leaving behind an isotopically enriched pool of dissolved inorganic carbon (DIC). Therefore, additional organic carbon burial should produce increasingly enriched DIC. Precipitation of calcium carbonate from this pool has little associated fractionation, allowing ancient carbonates to act as a tracer of organic carbon burial rates, and hence oxygen production (Knoll et al., 1986). Surprisingly, compiled carbonate records indicate that organic carbon burial has varied little over most of Earth history (Prokoph et al., 2008). This is not easily reconciled with evidence for orders of magnitude variation in oxygen concentration. Recent analyses of sediment organic carbon content (Sperling & Stockey, 2018) suggest a significant increase in organic carbon burial did occur in association with the Paleozoic oxygenation, contradicting traditional readings of the carbon isotope record.

Here, we explore possible explanations for this paradox, and suggest a new resolution based on the precipitation of authigenic carbonate. In particular, we propose that the precipitation of isotopically depleted authigenic carbonates is oxygen sensitive, and that this

Department of Earth and Planetary Sciences, Harvard University, Cambridge, Massachusetts, USA

Isotopic Constraints on Earth System Processes, Geophysical Monograph 273, First Edition.
Edited by Kenneth W. W. Sims, Kate Maher, and Daniel P. Schrag.

DOI:10.1002/9781119595007.ch08

forms a self-regulating system, in which the carbon isotope composition of seawater remains close to fixed value even under large variations in organic carbon burial and oxygen generation.

8.2. THE CARBON ISOTOPE BUDGET

The primary sources of inorganic carbon inputs to the ocean and atmosphere (F_{in}) are volcanism (V_C) and continental weathering of organic material (W_{org}) and carbonate minerals (W_{carb}). Dissolved inorganic carbon is transported to the ocean, where it can be removed by either photosynthetic carbon fixation or calcium carbonate precipitation. Much of this material is subsequently reoxidized or redissolved, but a portion is buried in sediments (B_{org}, B_{caic}), removing it from the ocean/atmosphere system until it is subducted or exposed to the atmosphere by sea level change or uplift.

At steady state, the carbon inputs and outputs must be balanced; $F_{in} = B_{org} + B_{carb}$. This is also true of the individual carbon isotopes, which, for a sufficiently rare isotope such as ^{13}C, yields:

$$\delta_{in} F_{in} = \delta_{org} B_{org} + \delta_{carb} B_{carb} \tag{8.1}$$

where δ_x is the δ^{13}C of burial flux B_x. The isotopic composition of carbonates is typically close to that of the dissolved pool from which it precipitates, while organic carbon is assigned an average offset of ε_{org}. Typically one assumes both phases are drawn from the same DIC pool, presumably seawater, though we revisit this assumption here in the context of authigenic carbonate precipitation in sedimentary porewaters. Given seawater δ^{13}C of δ:

$$\delta_{in} F_{in} = \left(\delta - \varepsilon_{org}\right) B_{org} + \delta B_{carb} \tag{8.2}$$

In order to make further progress, it is necessary to make some assumption about the isotopic composition of carbon inputs to the ocean, δ_{in}, over time. One approach is to assume it is constant over time at roughly its modern value, arguably reflecting the average composition of the crust or bulk Earth (e.g. Derry & France-Lanord, 1996; Hayes et al., 1999) in order derive the organic fraction of carbon burial on the seafloor:

$$f_{org} = \frac{\delta - \delta_{in}}{\varepsilon_{org}}; f_{org} = \frac{B_{org}}{F_{in}} \tag{8.3}$$

Assuming stable values of the fractionation ε_{org}, it is possible to derive variations in f_{org}, the organic proportion of total carbon burial, from the isotope record in carbonate minerals (Fig. 8.1).

Compilations of carbonate δ^{13}C over Earth history (Fig. 8.1) are characterized by mean values close to 0% over much of Earth history, suggesting that f_{org} has most frequently had values between 20% and 30%. Important exceptions include a period of unusually high variability in the Neoproterozoic, and extended periods of apparently elevated organic carbon such as the "Lomagundi excursion" from ~2400–2000 Ma, the Neoproterozoic, and the Carboniferous period, though the timing and size of these features does vary between data sets (e.g. Saltzman & Thomas, 2012).

8.3. f_{org} AND THE OXYGEN BUDGET

Oxygenic photosynthesis, likely the dominant mode of carbon fixation since at least the end of the Archean and possibly well before that time (e.g., Farquhar et al., 2011), produces both organic carbon and oxygen in a roughly 1:1 ratio, with an approximate stoichiometry of $CO_2 + H_2O + h\upsilon \rightarrow O_2 + CH_2O$. Today, the vast majority of the organic carbon produced in the ocean (> 99.9‰; Hedges & Keil, 1995) is re-oxidized while settling through the water column or in the upper few centimeters of the sediment on the ocean floor. Oxidation may be directly with O_2, essentially running the preceding reaction in reverse, or by alternative oxidants such as nitrate, iron, or sulfate, whose reduced by-products are themselves largely oxidized by O_2. As such, "long-term" oxygen production – production relevant on timescales longer than the mixing time of the ocean – is sometimes equated with the burial of organic carbon, or its reduced diagenetic by products, deep in marine sediments where it can be effectively sequestered from surface oxidant pools for tens of millions of years.

In a steady-state carbon cycle, the global rate of organic carbon burial and oxygen production is equal to the product of f_{org} and the rate of carbon input to the ocean. Assuming the latter is relatively constant over time, the carbon isotopic composition of carbonate in sedimentary rocks represents a record of oxygen production on long timescales (Knoll et al., 1986).

It has been argued that extended periods of elevated f_{org} represent accumulation of a large organic carbon reservoir and thus accumulation of O_2 in the atmosphere (Des Marais et al., 1992). This is consistent with redox proxy records (Fig. 8.1) that show a major increase in surface O_2 concentrations at the end of the Archean eon (Farquhar et al., 2001) and a second permanent rise, possibly in several stages, between the Ediacaran and the later Paleozoic (Lyons et al., 2014; Sperling et al., 2015).

However, steady-state oxygen concentrations are not set by the rate of oxygen production as recorded in f_{org}. Rather, they are the result of oxygen-sensitive sources and sinks adjusting until a balanced budget is achieved. A transient increase in oxygen concentrations, for example, should lead to more rapid oxygen consumption and a return to lower values on time scales related to the oxygen residence time of < 10 million years. This is in conflict with the apparently permanent oxygenation events recorded in redox proxies.

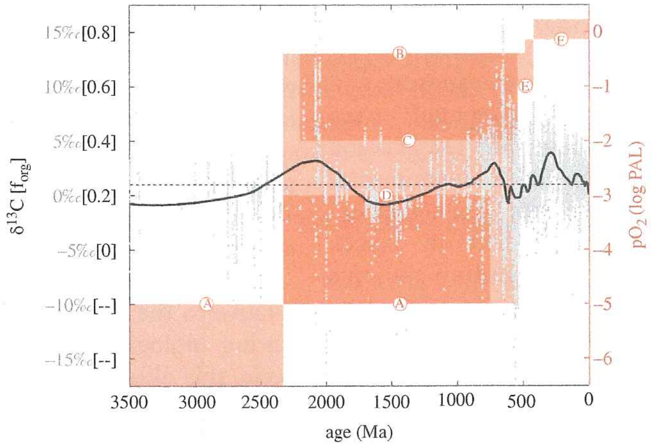

Figure 8.1 Variations in f_{org} and atmospheric pO_2 over Earth history as inferred from proxy records. f_{org} (black) has been calculated from a Loess smooth of the δ^{13}C record of carbonates (gray) compiled by Prokoph et al. 2008 following equation 8.3, assuming $\delta_{in} = -5$, $\varepsilon_{org} = 25$ The dashed line shows the average f_{org} calculated rom the entire carbonate data set. Proxy constraints on pO_2 are shown as red blocks; darker colors are used to illustrate disagreements between two proxy records. A: The presence of mass independent fractionation of sulfur isotopes in sediments older than ~2.4 Ga suggests pO_2 was less than 10^{-5} present atmospheric levels (PAL; Pavlov & Kasting, 2002) at that time, and subsequently exceeded that value. B: The presence of an anoxic deep ocean through the Cambrian (488 Ma; Sperling et al. 2015) has been inferred to require atmospheric pO_2 below 40% PAL (Canfield, 1998). C: Iron enrichments in paleosols suggest a lower bound on O_2 during this period of ~1% PAL (Rye & Holland, 1999); D: chromium isotope enrichments suggest an incompatible upper bound of ~0.1% PAL (Planavsky et al., 2014) until 750 Ma. E: The body plans and motility of Cambrian fauna (< 540 Ma) is thought to require oxygen levels about 10% PAL (Sperling et al., 2013). F: The loss of persistent anoxia sometime after the Ordovician gives a new upper bound of 70‰ based on the lack of charcoal deposits (Belcher & McElwain, 2008) until the latest Silurian (Glasspool et al., 2004), after which a continuous charcoal record limits pO_2 to 70% to 170% PAL (Lenton & Watson, 2000).

Put differently, the apparent constancy of f_{org} over most of Earth history implies a stable rate of O_2 production that must have been balanced by a similarly stable consumption rate. It is not obvious that this is possible: most oxygen sinks scale monotonically with pO_2, which has varied by many orders of magnitude over Earth history. In particular, low oxygen concentrations in the early Paleozoic, and certainly in the Precambrian, should have led to much smaller oxygen sinks and an unbalanced O_2 budget. We review this paradox in more detail in Section 8.4, considering whether any of the major redox-sensitive elements could have balanced cycles under low oxygen conditions that consume O_2 as rapidly as they do today. We will first demonstrate this is not possible, and that the Precambrian oxygen budget must have been characterized by low rates of organic carbon burial, calling into question our understanding of the δ^{13}C record in carbonates. We will then consider alternative readings of this isotope record in an effort to resolve the f_{org} / O_2 paradox.

8.4. OXYGEN SINKS IN A LOW-OXYGEN WORLD

By balancing the production of oxygen through organic carbon burial against oxidative sinks, the oxygen budget can be written as:

$$B_{org} = W_{org} + \Sigma S_{ox} + \Sigma Fe_{ox} + \Sigma e^{-} \tag{8.4}$$

where ΣX_{ox} is the net oxidation of a redox-sensitive element X on the Earth's surface, the most quantitatively significant of which are sulfur and iron; and Σe^{-} represents total oxidation of other minor species, such as H_2 derived from serpentinization and volcanism. We consider each of the sink terms on the right-hand side in turn, and ask whether, even during low-oxygen portions of Earth history, they could collectively balance the constant, modern levels of organic carbon burial implied by the carbon isotope record.

8.4.1. Carbon as a Precambrian Oxygen Sink

Marine burial of organic carbon, as recorded in f_{org}, is the major oxygen source, but subsequent exposure and oxidative weathering of this material during uplift or sea level change is a quantitatively important oxygen sink (e.g. Hayes & Waldbauer, 2006). Both experimental (Chang & Berner, 1999) and modeling (Daines et al., 2016) studies find this rate is dependent on oxygen concentration in the atmosphere, suggesting the rate should indeed have been lower in the Precambrian, contributing to an apparently unbalanced oxygen budget.

A decreased rate of organic carbon weathering would, however, increase the C isotopic composition of rivers, leading to an overestimate of f_{org} if assuming modern values and possibly reconciling the record (Daines et al., 2016). It is possible to discard the assumption of constant δ_{in} by instead assuming that, because the weathering reservoirs of carbonate and organic carbon are derived from ancient, uplifted sediments, they are likely to have a similar isotopic composition on tectonic timescales. One can then decompose the input flux into its constituent parts to arrive at an alternative definition of f_{org} not dependent on δ_{in}:

$$f^*_{org} = \frac{\delta - \delta_V}{\varepsilon_{org}};\ f^*_{org} = \frac{B_{org} - W_{org}}{V_C} \tag{8.5}$$

Unlike f_{org}, which represents the organic proportion of carbon burial on the seafloor, f^*_{org} is the organic proportion of *net* carbon removal from the Earth surface – that is, the difference between organic weathering and burial. Given that the isotopic composition of volcanic inputs has likely not varied over Earth history, the carbonate record again suggests that oxygen production associated with carbon cycling, now in a net rather than gross sense, has not changed even as oxygen levels varied by orders of magnitude. At steady state, this production must be balanced by net oxidation of sulfur, iron, or other redox-sensitive elements, the global rates of which are likely oxygen sensitive. Therefore, regardless of which interpretation of the carbonate record one prefers, a fundamental paradox remains.

8.4.2. Sulfur as a Precambrian Oxygen Sink

Sulfur interacts with the oxygen cycle primarily through biological oxidation and reduction:

$$SO_4^{2-} + 2H^+ \leftrightarrow H_2S + 2O_2 \tag{8.6}$$

The oxidized form, sulfate, can be removed from the oceans by precipitation of sulfate minerals, particularly gypsum in evaporites. The reduced phase, hydrogen sulfide, can be partially oxidized by various electron acceptors and precipitate as pyrite. These are the primary modes of sulfur burial in the ocean, and are largely balanced by subaerial weathering of the same, with a minor source from volcanism and hydrothermal activity. Net burial of pyrite therefore represents a source of oxygen, while net burial of sulfate minerals is a sink.

Unlike sulfate minerals, pyrite is isotopically depleted relative to the seawater sulfur pool due to fractionation during biological sulfate reduction. As in the carbon cycle, this allows for a mass balance approach for estimating their relative contributions to burial. The canonical result is that pyrite accounts for approximately 40% of sulfur burial today (Canfield 2004), with the remainder assumed to be in evaporite deposits. Uncertainties in the calculation, and the lack of steady state in the present day, allow for an average Cenozoic f_{py} ranging from 10% to 90% (Halevy et al., 2012; Tostevin et al., 2014). The relative rates of pyrite and evaporite weathering are also quite uncertain (Burke et al., 2018), making a net oxygen effect difficult to calculate directly from observed quantities.

Nevertheless, the Phanerozoic sulfur cycle is most likely a net sink for oxygen. In theory, the transfer of sulfur from subaerial gypsum deposits to marine pyrite could represent a source of oxygen, but evaporite deposits – highly soluble and subject to inundation – are geologically short lived, with few quantitatively important deposits now extant (Holser et al., 1988). A significant net reduction of sulfur during the later Phanerozoic would somehow require continuous weathering and subsequent reduction of massive evaporites accumulated in the Ediacaran or early Paleozoic, when bedded sulfur evaporites first appear. Rather, oxidation and burial of sulfur sourced from Precambrian pyrites, or from mantle sulfide and sulfite, must represent a net sink for oxygen, however small.

Under the low-oxygen conditions of the Precambrian, pyrite was the dominant mode of sulfur removal from the ocean. The scarcity of Precambrian sulfate evaporites (Evans, 2006), mass balance considerations (Canfield, 2004), and isotopic evidence for low sulfate concentrations before the Ediacaran (Halverson & Hurtgen, 2007) are all consistent with a dominant and efficient pyrite sink. This may have been due to several effects, including: abundant substrates for sulfate reduction given limited competition from oxic respiration (Westrich & Berner, 1984); low rates of sulfide reoxidation in an oxygen-poor environment lacking vigorous bioturbation (Canfield & Farquhar, 2009); and increased availability of iron in a ferruginous ocean (Sperling et al., 2015).

Given a predominantly pyritic burial flux, weathering must also have been dominated by pyrite oxidation. This implies that weathering and burial were largely a net-zero redox cycle, with net oxidation of sulfur limited to oxidation of hydrothermal sulfides to pyrite. Barring significant changes in hydrothermal flows since the late Archean (Holland, 2002), the rate of net sulfur oxidation would have been at or near its theoretical minimum in the Precambrian, and necessarily smaller than it is today.

8.4.3. Iron as a Precambrian Oxygen Sink

Iron is also redox sensitive. The quantitatively important phases in the surface redox cycle are insoluble, oxidized ferric iron minerals and soluble, reduced ferrous iron:

$$4FeOOH + 8H^+ \leftrightarrow 4Fe^{2+} + O_2 + 6H_2O \tag{8.7}$$

where goethtite, FeOOH, has been used to represent a suite of possible ferric oxides. Ferrous iron may precipitate from the ocean as a component of pyrite, or in ferrous phosphate (vivianite), -silicate (greenalite), or -carbonate (ankerite). The source of iron today is dominated by oxidative weathering of a mixed-valence continental source, which is transported to the oceans overwhelming as particulate oxides (e.g. Poulton & Raiswell, 2004). These oxides are reduced and reoxidized in sediment, but burial of ferrous phases other than pyrite are relatively rare. Riverine iron fluxes are an order of magnitude larger than sulfur fluxes (Burke et al., 2018; Poulton & Raiswell, 2004; Walker & Brimblecombe, 1985), suggesting that pyrite cannot play a major role in iron removal, and therefore the modern iron cycle is characterized by net oxidation.

Precambrian iron burial was almost certainly less oxidized, though quantitative constraints are few. Iron-depleted paleosols in the Archean and the Proterozoic are inferred to reflect loss of soluble reduced iron during weathering (Rye & Holland, 1999), while higher rates of pyrite burial (see Section 8.4.2) require additional burial of reduced iron. Iron speciation data suggests that the deep water column was ferruginous through most of the Precambrian (Poulton & Canfield, 2011) and into the Paleozoic (Sperling et al., 2015), which most likely promoted burial of reduced iron minerals that are rare in the modern ocean, such as greenalite or vivianite (e.g. Derry, 2015). Each observation points to less net oxidation than is seen today.

A recent study of island arc basalts suggests that the continental iron source may have been more reduced before the Phanerozoic (Stolper & Bucholz, 2019). While this implies increased oxygen loss during Precambrian weathering, the oxidation of Phanerozoic basalt is argued to derive from subduction of oxygen-rich surface reservoirs, and therefore there is no net change in oxygen consumption – simply a change in locality, from subaerial to subduction zone.

8.4.4. Other Precambrian Oxygen Sinks

Reducing fluids derived from the mantle act as oxygen sinks when exposed to surface reservoirs through volcanism and hydrothermal activity. The reducing power may be carried in a number of chemical forms, but hydrogen derived from fluids or from serpentinization of seafloor basalt is a representative and quantitatively significant carrier (e.g. Bach & Edwards, 2003):

$$2H_2 + O_2 \leftrightarrow 2H_2O \tag{8.8}$$

Today these reductants are oxidized almost immediately; both hydrogen and its abiotic products, such as methane, have extremely short residence times in the ocean and atmosphere (e.g. Olson et al., 2016). Therefore, this sink is at its maximum possible value, given the rate and redox state of outgassing.

The redox state of these fluids is unlikely to have been substantially different from today after the late Archean, as the mantle redox state stabilized by 3.0 Ga (Li & Lee, 2004) and craton formation finished by ~2.5 Ga, limiting major changes in the average pressure in hydrothermal systems (Holland, 2002). Higher heat flow at earlier stages in Earth history (Turcotte, 1980) could have led to increased outgassing rates (e.g. Canfield, 2004), but also may have limited the formation of slow, cool spreading centers in which serpentinization occurs today (Sleep et al., 2004). Furthermore, increased carbon outflow also ultimately leads to more rapid weathering rates (Walker et al., 1981), additional nutrient input, and more rapid oxygen production (Bergman et al., 2004; Laakso & Schrag, 2017). In sum, non-sulfur and non-iron reductants are not likely to have been significantly larger sinks for O_2 in the Proterozoic or the latest Archean.

8.5. RESOLVING THE pO_2 - f_{org} PARADOX

Each of the major redox-sensitive element cycles – carbon, sulfur, iron, and hydrogen – are likely to have been smaller net oxygen sinks during the Proterozoic and late Archean than they are today. This suggests that the stable low oxygen levels of the Precambrian were only possible if the oxygen source associated with organic carbon burial were smaller than today.

One explanation for a shift in oxygen production is that the total flux of carbon through the Earth's surface was smaller at earlier portions of Earth history (Husson & Peters, 2017; Lee et al., 2016; Shield & Mills, 2017; Williams et al., 2019). This hypothesis allows for a smaller *absolute* rate of oxygen production while maintaining a constant burial *fraction,* f_{org}, consistent with the conventional reading of the carbon isotope record in carbonates. However, this hypothesis requires permanently sustained increases in surface carbon fluxes. There is some evidence for increased total burial during the Phanerozoic relative to the Precambrian (Husson & Peters, 2017), but this data can also be explained by simple erosion rather than permanent depositional shifts (Keller et al., 2019). There may have been an increase in carbon input via outgassing following the Cryogenian glaciations (see Williams et al., 2019, for discussion), but these do not obviously show a systematic difference between the poorly oxygenated Proterozoic and the well-oxygenated Phanerozoic. We therefore take the perspective that total carbon fluxes have remained roughly constant.

However, as argued by Schrag et al. (2013), the conventional mass balance interpretation of the carbon isotope record neglects an important mode of burial: authigenic carbonate. These are carbonate minerals precipitated in marine sediments, adopting the isotopic composition of porewater DIC. Porewaters can be significantly isotopically fractionated relative to seawater, primarily due to oxidation of depleted organic carbon and methane. When the oxidation is coupled to reduction of sulfate or iron, alkalinity increases, leading to supersaturation and potential precipitation of isotopically depleted carbonate minerals. Today, such carbonates can have $\delta^{13}C$ values depleted by 60‰ relative to seawater, though more typically 10–15‰ (Meister et al., 2007; Naehr et al., 2007).

The key characteristic of these carbonates in the context of carbon isotope records is that they do not reflect the $\delta^{13}C$ of seawater DIC. We use the term "authigenic carbonates" to describe these minerals, implying precipitation in the sediment column, but they may also include early diagenetic recrystallization of primary marine precipitates that adopt porewater-influenced values (Higgins et al., 2018), or even seafloor precipitates influenced by diffusion from below. Any isotopically depleted inorganic carbon sink will allow for enrichment of the other surface reservoirs without affecting the oxygen budget. It is well documented that precipitation of carbonate minerals on the seafloor declined from Archean to Ediacaran time (Grotzinger & James, 2000) even as oxygen levels increased (e.g. Lyons et al., 2014). Motivated by this observation, we suggest that oxygen-sensitive precipitation of isotopically depleted authigenic carbonate minerals leads to a negative feedback that sustains marine DIC near a constant $\delta^{13}C$ value. As this isotopic composition will be recorded in primary marine precipitates that are much more likely to preserved in well-studied, shallow water carbonate platforms than authigenic material (Schrag et al., 2013), the result will be a stable $\delta^{13}C$ record in carbonates and an apparently constant value of f_{org}.

Precipitation of sedimentary carbonates requires supersaturation of carbonate minerals in porewaters, typically associated with higher pH values. This can be the result of supersaturation in the overlying water column, or of alkalinity generation during diagenesis (e.g. Bergmann et al., 2013); both effects are likely sensitive to the oxygen content of the global ocean.

Today, deeper portions of the water column (thousands of meters) are generally undersaturated, leading to dissolution of carbonate in underlying sediments (e.g. Key et al., 2004). This is due in part to temperature and pressure effects, but an additional important control is the "biological pump": the sinking and subsequent remineralization of photosynthetically derived organic material decreases both pH and carbonate saturation in the deep ocean. However, a suboxic water column is less efficient at remineralizing organic material (Van Mooy et al. 2002), and anoxic water bodies even less so (Kuntz et al. 2015). As a result, low-oxygen periods of Earth history were likely characterized by weaker gradients in pH and carbonate saturation, leading to supersaturation over large swaths of the ocean floor than during oxygenated intervals (Higgins et al., 2009). This mechanism may explain the decline in seafloor precipitates as oxygen levels rose over the Precambrian (Higgins et al., 2009). These oxygen-mediated changes in the structure of the ocean's saturation state are consistent with modern seafloor environments that produce authigenic carbonate slowly relative to biogenic production (Mitnick et al., 2018; Sun & Turchyn, 2014). Indeed, our hypothesis requires a reduced role for authigenic carbonates in the Phanerozoic carbon cycle, consistent with modern observations of an ocean dominated by primary marine precipitates.

Furthermore, increases in ocean oxygen concentration, or in the area of oxygenated sediments, permit more extensive oxic remineralization (e.g. Katsev & Crowe, 2015). This process generates a low pH lens in the upper sediment column and limits access to labile organic substrates for alkalinity generating metabolisms such as iron and sulfate reduction (Westrich & Berner, 1984), suppressing the carbonate saturation state (Bergman et al., 2004). This combination of effects suggests that that global rate of authigenic carbonate is likely sensitive to the oxygen content of the ocean. As argued earlier, oxygen concentrations most likely increase when there is an increase in the burial of isotopically depleted organic carbon, mediated by changes in phosphorus supply (Laakso & Schrag, 2017). The rise in pO_2 suppresses precipitation of isotopically depleted authigenic carbonate, as an increase in oxic respiration takes place at the expense of alkalinity generating organisms, and reduces the area of carbonate saturated seafloor by enhancing the biological pump. The net effect is opposing changes in the total burial of isotopically depleted carbon phases, with competing effects on the $\delta^{13}C$ of the residual marine DIC pool and suppressed variability compared to that expected from changes in f_{org} alone.

8.6. PREDICTIONS OF THE AUTHIGENIC FEEDBACK HYPOTHESIS

How large a change in organic carbon burial could be masked in the carbon isotope record by changes in authigenic carbonate formation? Following Schrag et al. (2013), the C isotope mass balance can be expanded to include burial of authigenic carbonate:

$$\delta_{in} = \left(\delta - \varepsilon_{org}\right) f_{org} + \left(1 - f_{org}\right)\left(\left(\delta - \varepsilon_{auth}\right) f_{auth} + \delta\left(1 - f_{auth}\right)\right) \tag{8.9}$$

Where f_{auth} is defined as the authigenic fraction of total carbonate burial and ε_{auth} is the average isotopic offset of authigenic carbonate relative to seawater. Here we assume a constant value of δ_{in}; however, if changes in the ratio of authigenic to primary carbonate affect the probability of recycling – not implausible given the different environments in which these form (Schrag et al., 2013) – then riverine inputs may change over time. In this case, the following arguments are better applied to f^*_{org} and an equivalent definition of f^*_{auth}, i.e., the net of burial and weathering rather than gross burial (see Section 8.2). The conceptual argument, however, remains the same.

Solving for f_{auth}:

$$f_{auth} = \frac{\left(\delta - \delta_{in}\right) - \varepsilon_{org} f_{org}}{\left(1 - f_{org}\right)\varepsilon_{auth}} \tag{8.10}$$

If we assume, as in the modern, $\delta_{in} \sim 5‰$, $\varepsilon_{org} \sim 25‰$, and $\varepsilon_{auth} \sim 15‰$, then seawater DIC and marine carbonates can maintain $\delta = 0‰$ even if f_{org} is zero; this requires that authigenics make up one-third of all carbonate burial (Fig. 8.2). Though the conventional mass balance does not include authigenic carbonate, it is estimated to account for at least 10‰ of modern burial (Sun & Turchyn, 2014). Therefore, the changes in authigenic precipitation required to account for even major changes in organic carbon burial are only on the scale of factors of two, rather than orders of magnitude.

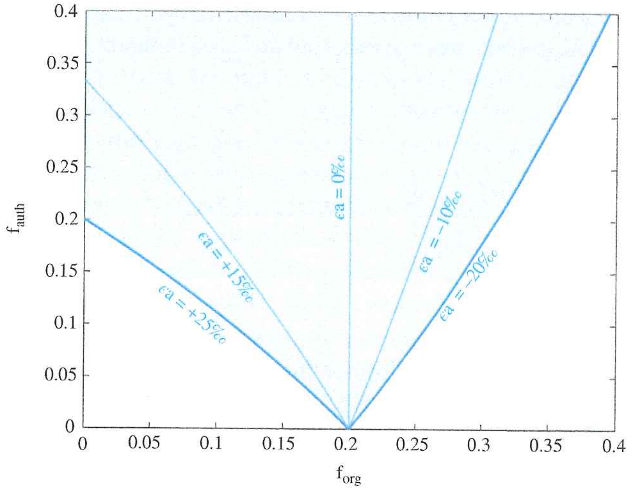

Figure 8.2 Carbon cycle parameters consistent with a steady state seawater $\delta^{13}C$ value of 0‰. The steady state isotopic composition of marine DIC as a function of the organic fraction of total carbon burial (f_{org}) and the authigenic fraction of carbonate burial (f_{auth}). The blue field shows the set of f_{org} and f_{auth} combinations that yield physically plausible solutions, given potential variations in the isotopic composition of authigenic carbonate relative to seawater. The arcs represent a single value for that isotopic offset, ranging from remineralization-dominated ($\varepsilon_a = \varepsilon_{auth} = +25‰$) to methanogenesis-dominated ($\varepsilon_{auth} = -20‰$). ε_{org} is fixed at +25‰.

More generally, we are interested in the conditions under which the oxygen sensitivity of authigenic carbon precipitation will mask variability in organic carbon burial by suppressing changes in seawater $\delta^{13}C$. We can define the "observed" f_{org} derived from the marine carbonate as $f_{obs} = (\delta - \delta_{in})/\varepsilon_{org}$, following equation 8.3. Assuming for a moment that the *average* fractionation factors ε_{org} and ε_{auth} are roughly stable near typical modern values of 25‰ and 15‰ – though this needn't be the case for authigenics – we can restate the authigenic-corrected mass balance 8.9 in terms of f_{obs} and take the derivative with respect to f_{org}:

$$\frac{d\left(f_{obs}\right)}{d\left(f_{org}\right)} = \left(1 - f_{auth}\frac{\varepsilon_{auth}}{\varepsilon_{org}}\right) + \left(1 - f_{\text{arg}}\right)\frac{\varepsilon_{auth}}{\varepsilon_{org}}\frac{d\left(f_{auth}\right)}{d\left(f_{org}\right)} \tag{8.11}$$

The first term represents reduced variability in seawater $\delta^{13}C$ that results simply from the presence of authigenic carbonate in the mass balance, though at the estimated modern value of $f_{auth} \sim 10\%$, this effect will be small. The second term captures the trade-off between isotopically depleted authigenic carbonate and isotopically depleted organic carbon: at steady state, larger f_{org} implies higher oxygen concentrations, and hence a reduction in f_{auth}. As a result, the change in f_{obs} is always smaller than the change in f_{org}, i.e. $df_{obs}/df_{org} < 1$. (This would not be true if global authigenic carbonate were isotopically enriched, $\varepsilon_{auth} < 0$, which is possible in rare modern settings dominated by methanogenesis.)

This effect will completely decouple oxygen variability from the carbon isotope record if $d(f_{obs}) = 0$, which occurs when

$$\left.\frac{d\left(f_{auth}\right)}{d\left(f_{org}\right)}\right|_{d(f_{obs})=0} = \frac{f_{auth} - \left(\frac{\varepsilon_{org}}{\varepsilon_{auth}}\right)}{1 - f_{org}} \tag{8.12}$$

Following the Devonian, oxygen concentrations have remained consistently higher than in the early Paleozoic or the Precambrian (e.g. Sperling et al., 2015). This suggests that modern f_{org} is likely near its historical maximum at 15% (for $f_{auth} = 10\%$, $\varepsilon_{auth} = 15‰$). f_{auth} is also small relative to $\varepsilon_{org}/\varepsilon_{auth}$, suggesting that, at least in the later Phanerozoic, the critical condition can be simplified to:

$$\left.\frac{d\left(f_{auth}\right)}{d\left(f_{org}\right)}\right|_{d(f_{obs})=0} \approx -\frac{\varepsilon_{org}}{\varepsilon_{auth}} \approx -1.7 \tag{8.13}$$

These results are summarized in Fig. 8.3, which shows the value of seawater $\delta^{13}C$ (δ) after changes in f_{org} and f_{auth}, compared changes with fixed f_{auth}; these calculations assume $\delta = 0‰$ for $f_{org} = 15\%$, $f_{auth} = 10\%$, and $\varepsilon_{auth} = 15‰$.

Taking the Paleozoic oxygen increase as an example, modeling suggests that a four-fold increase in pO_2 was induced by a doubling of organic carbon burial (Bergman et al., 2004), and compiled data on sedimentary organic carbon content (Stockey & Sperling, 2018) is consistent with a large increase in organic carbon burial beginning as early as the Cambrian. Though seawater $\delta^{13}C$ may increase somewhat across this transition, carbon isotope compilations show a much smaller change than would be expected purely from a doubling of carbon burial. Following equation 8.13, suppressing *any* increase would therefore require a roughly 3- to 4-fold decrease in authigenic carbon through this transition, assuming its isotopic composition did not undergo any drastic change. This makes a testable prediction for the sensitivity of authigenic carbonate precipitation to oxygen levels. The response to changes in the biological pump (Higgins et al., 2009) is necessarily an ocean-scale effect that can only be studied in a paleoceanographic context. However, the local effect of O_2 on alkalinity generation can be tested through observational studies of modern low-oxygen settings.

Calcium isotopes provide one test of the hypothesis. Seawater carbonate precipitates are typically depleted in ^{44}Ca relative to seawater: biogenic calcite and aragonite have average $\delta^{44/40}Ca$ offset of −1.3‰ and −1.7‰, respectively (Blättler et al., 2012). If such precipitates are the dominant calcium sink, a steady-state Ca cycle should yield an ocean enriched by 1–2‰, relative to river inputs. However, equilibrium fractionation between seawater and calcium carbonate is approximately 0‰ (Fantle & DePaolo, 2007), and this is realized at the slow formation rates typical of sedimentary recrystallization and authigenic precipitation (Fantle & DePaolo, 2007). As argued by Mitnick et al. (2018) and Higgins et al. (2018), more extensive formation of carbonates in the upper, fluid buffered sediment column will yield a calcium sink that is more isotopically similar to seawater, depressing steady-state $\delta^{44/40}Ca$ in seawater and primary marine carbonates.

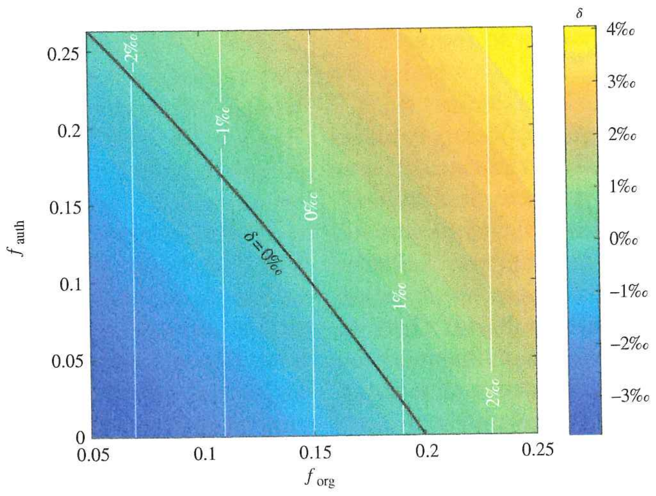

Figure 8.3 Variation in the $\delta^{13}C$ of seawater and primary marine carbonates (δ; colored contours) with changes in f_{org} and f_{auth}. Calculations are based on a "modern" steady-state carbon cycle with $\delta = 0‰$, $f_{org} = 0.15$, $\varepsilon_{org} = 20‰$, and $\varepsilon_{auth} = 15‰$, requiring $f_{auth} = 0.098$ (Based on Sun, 2014). The black contour shows a constant value of $\delta = 0‰$. The white contours show variations in $\delta^{13}C$ assuming f_{auth} is constant at a value of 0.098.

Balancing a constant river input against two sinks with their own average fractionation factors allows us to calculate the sensitivity of $\delta^{44/40}Ca$ in seawater and marine precipitates to changes in the authigenic fraction of global carbonate precipitation:

$$\frac{d\left(\delta^{44/42}\mathrm{Ca}_{\mathrm{mar}}\right)}{d\left(f_{auth}\right)} = \varepsilon_{\mathrm{auth}}^{\mathrm{Ca}} - \varepsilon_{\mathrm{mar}}^{\mathrm{Ca}} \approx 1.3 \tag{8.14}$$

where ε^{Ca} is the average calcium isotopic offset between seawater and a carbonate phase; we have assumed $\varepsilon_{\mathrm{mar}}^{\mathrm{Ca}} = -1.3\%$ and $\varepsilon_{\mathrm{auth}}^{\mathrm{Ca}} = 0\%$. As an example, consider the Paleozoic oxygenation discussed previously, during which oxygen levels increase in the Silurian and/or Devonian with a possible peak in the Carboniferous (see Krause et al., 2018, for a recent summary). According to our hypothesis, maintaining a constant value of seawater $\delta^{13}C$ requires f_{auth} to fall from ~25% to ~10%. Following equation 8.14, the $\delta^{44/40}Ca$ of primary marine carbonates should increase by 0.2‰ across the Paleozoic oxygen event. This is consistent with observations, which show an increase of 0.7‰ from the Devonian to the late Carboniferous (Blättler et al., 2012). The effect we have described here is too small to explain the entire signal; other factors, notably a change in the dominant mineralogy of marine precipitates almost certainly played a role (Blättler et al., 2012; Farkaš et al., 2007). Nevertheless, a decrease in authigenic carbonate precipitation during the Paleozoic oxygenation can explain both the relatively small signal in $\delta^{13}C$ and an apparent rise in $\delta^{44/40}Ca$ that is not repeated during subsequent oscillations between aragonite- and calcite-dominated periods of the record (Blättler et al., 2012).

This hypothesis also predicts substantial changes in the scale of authigenic carbonate deposition, which might be directly observable. A major challenge to making such observations is that, by definition, it assumes that the observed carbon isotope record is dominated by marine carbonates, and that the predicted authigenic carbonates are not well observed. This requires that the authigenic carbonates precipitated in sediments that are consistently undersampled (Schrag et al., 2013). Given that authigenic carbonates are most likely to precipitate in organic-rich, oxygen-poor sediments with rapid rates of sulfate and iron reduction, it is possible that they occurred in anoxic Neoproterozoic slope sediments (Sperling et al., 2015) that are less likely to be included in $\delta^{13}C$ compilations than thick, shallow-water carbonate platforms. We therefore predict that Precambrian carbonates found as a minor phase in deeper water, organic carbon-rich shales should be isotopically depleted relative to platform carbonates and may bear calcium and magnesium isotope signatures characteristic of authigenic precipitation or early diagenetic recrystallization (Higgins et al., 2018). A recent compilation of clastic-hosted carbonates (Canfield et al., 2020) did find evidence for remineralization-influenced diagenetic carbonates across the later Neoproterozoic. While promising, the data does not contain any changes in the sign of the isotopic offset across any major perturbation. Furthermore, the authors conclude that, if the concentrations and isotopic compositions they observe are representative, authigenic precipitation is unlikely to have had a substantial effect on the global carbon mass balance. While an important first step, this data represents a handful of sites of varying depositional setting; additional samples will be necessary to further test the hypothesis, with a more systematic emphasis on organic-rich deep water formations. More extensive sampling may be even more important for Proterozoic clastic sediments if overall organic matter burial was more limited and primary production was more limited by nutrient availability (Laakso & Schrag, 2018). In the modern ocean, high primary production leads to a broader distribution of organic-rich sediments, such that many clastic sediments have significant organic matter content. This would not be true in the Proterozoic, if primary production was much more limited, focused in locations with phosphorous inputs. This implies a more uneven distribution of organic matter and hence authigenic carbonate.

8.7. CONCLUSIONS

We propose that the $\delta^{13}C$ of seawater DIC is controlled by an oxygen-sensitive rate of authigenic carbonate precipitation, which both explains the constancy of carbonate $\delta^{13}C$ over time and decouples this value from the rate of organic carbon burial. This resolves the apparent paradox of constant oxygen generation across time periods characterized by enormous changes in oxygen concentration. However, it suggests that the carbon isotope record is not a simple record of oxygen cycling.

This hypothesis also has implications for periods of earth history when the carbon isotope record is not close to its "average" value of 0‰. Periods of extended enrichment, such as the Lomagundi excursion of the Paleoproterozoic or the Ediacaran, may be explained in part by net oxygen generation, but may also record periods of enhanced authigenic burial. Similarly, the massive negative excursions of the Neoproterozoic and Cambrian could represent some combination of organic carbon oxidation, local emplacement of depleted authigenic carbonate, or off-shore precipitation of enriched authigenic carbonates. Identifying reliable means of disentangling these effects remains a major challenge. Advances in petrography (Husson et al., 2015) and calcium and magnesium isotope analysis (Blättler et al., 2015) are promising, but testing any new hypothesis will likely require expansion of carbon isotope records to unconventional deeper water settings that are poorly preserved and suffer from poor stratigraphic control. Nevertheless, the inclusion of authigenic carbonate in carbon isotope mass balance suggests new solutions to a number of major problems in biogeochemical cycles over Earth history.

REFERENCES

Bach, W., & Edwards, K. (2003). Iron and sulfide oxidation within the basaltic oceanic crust: chemolithoautotrophic microbial biomass production. *Geochimica et Cosmochimica Acta*, *67*, 38713887. https://doi.org/10.1016/S0016-7037(03)00304-1

Belcher, C., & McElwain, J. (2008). Limits for combustion in low O_2 redefine paleoatmospheric predictions for the Mesozoic. *Science*, *321*, 1197–1200. doi:10.1126/science.1160978

Bergman, N., Lenton, T., & Watson, A. (2004). COPSE: A new model of biogeochemical cycling over Phanerozoic time. *American Journal of Science*, *304*, 397–437. https://doi.org/10.2475/ajs.304.5.397

Bergmann, K., Grotzinger, J., & Fischer, W. (2013). Biological influences on seafloor carbonate precipitation. *Palaios*, *28*, 99–115. http://dx.doi.org/10.2110/palo.2012.p12-088r

Blättler, C., Miller, N., & Higgins, J. (2015). Mg and Ca isotope signatures of authigenic dologmite in siliceous deep-sea sediments. *Earth and Planetary Science Letters*, *419*, 32–32. https://doi.org/10.1016/j.epsl.2015.03.006

Blättler, C., Henderson, G., & Jenkyns, H. (2012). Explaining the Phanerozoic Ca isotope history of seawater. *Geology*, *40*, 843–846. https://doi.org/10.1130/G33191.1

Burke, A., Present, T., Paris, G., Rae, E., Sandilands, B., Gaillardet, J., et al. (2018). Sulfur isotopes in rivers: Insights into global weathering budgets, pyrite oxidation, and the modern sulfur cycle. *Earth and Planetary Science Letters*, *496*, 168–177. https://doi.org/10.1016/j.epsl.2018.05.022

Canfield, D. (1998). A new model for Proterozoic ocean chemistry. *Nature*, *396*, 450–453. https://doi.org/10.1038/24839

Canfield, D. (2004). The evolution of the Earth surface sulfur reservoir. *American Journal of Science*, *304*, 839–861. https://doi.org/10.2475/ajs.304.10.839

Canfield, D., & Farquhar, J. (2009). Animal evolution, bioturbation, and the sulfate concentration of the oceans. *Proceedings of the National Academy of Sciences of the USA*, *106*, 8123–8127. https://doi.org/10.1073/pnas.0902037106

Canfield, D., Knoll A., Poulton S., Narbonne, G., & Dunning G. (2020). Carbon isotopes in clastic rocks and the Neoproterozoic carbon cycle. *American Journal of Science*, *320*, 97–124. https://doi.org/10.2475/02.2020.01

Chang, S., & Berner, R. (1999). Coal weathering and the geochemical carbon cycle. *Geochimica et Cosmochimica Acta*, *63*, 3301–3310. https://doi.org/10.1016/S0016-7037(99)00252-5

Crockford, P., Hayles, J., Bao, H., Planavsky, N., Bekker, A., Fralick, P., Halverson, G., Bui, T., Peng, Y., & Wing, B. (2018). Triple oxygen isotope evidence for limited Proterozoic primary productivity. *Nature*, *559*, 613–616. https://doi.org/10.1038/s41586-018-0349-y

Daines, S., Mills, B., & Lenton, T. (2017). Atmospheric oxygen regulation at low Proterozoic levels by incomplete oxidative weathering of sedimentary organic carbon. *Nature Communications*, *8*. https://doi.org/10.1038/ncomms14379

Derry, L. (2015). Causes and consequences of mid-Proterozoic anoxia. *Geophysical Research Letters*, *42*, 8538–8546. https://doi.org/10.1002/2015GL065333

Derry, L., & France-Lanord, C. (1996). Neogene growth of the sedimentary organic carbon reservoir. *Paleoceanography*, *11*, 267–275. https://doi.org/10.1029/95PA03839

Des Marais, D., Strauss, H., Summons, R., & Hayes, J. (1992). Carbon isotope evidence for the stepwise oxidation of the Proterozoic environment. *Natures*, *359*, 605–609. https://doi.org/10.1038/359605a0

Evans, D. (2006). Proterozoic low orbital obliquity and axial-dipole geomagnetic filed from evaporite paleolatitudes. *Nature*, *444*, 51–55. https://doi.org/10.1038/nature05203

Fantle, M., & DePaolo, D. (2007). Ca isotopes in carbonate sediment and pore fluid from ODP Site 807A: the Ca^{2+}(aq)-calcite equilibrium fractionation factor and calcite recrystallization rates in Pleistocene sediments. *Geochimica et Cosmochimica Acta*, *71*, 2524–2546. https://doi.org/10.1016/j.gca.2007.03.006

Farkaš, J., Böhm, F., Wallmann, K., Blenkinsop, J., Eisenhauer, A., van Geldern, R., et al. (2007). Calcium isotope record of Phanerozoic oceans: Implications for chemical evolution of seawater and its causative mechanisms. *Geochimica et Cosmochimica Acta*, *71*, 5117–5134. https://doi.org/10.1016/j.gca.2007.09.004

Farquhar, J., Savarino, J., Airieau, S., & Thiemens, M. (2001). Observation of wavelength-sensitive mass-independent sulfur isotope effects during SO2 photolysis: implications for the early atmosphere. *Geophysical Research Letters: Planets*, *106*. https://doi.org/10.1029/2000JE001437

Farquhar, J., Zerkle, A., & Bekker, A. (2011). Geological constraints on the origin of oxygenic photosynthesis. *Photosynthesis Research*, *107*, 11–36. https://doi.org/10.1007/s11120-010-9594-0

Glasspool, I., Edwards, D., & Axe, L. (2004). Charcoal in the Silurian as evidence for the earliest wildfire. *Geology*, *32*, 383. https://doi.org/10.1130/G20363.1

Holser, W., Schidlowski, M., Mackenzie, F., & Maynard, J. (1988). Geochemical cycles of carbon and sulfur. In: C. Gregor, R. Garrels, F. Mackenzie, & J. Maynard (eds.), *Chemical Cycles in the Evolution of the Earth*, pp. 105–173), New York: Wiley.

Grotzinger, J., & James, N. (2000). Precambrian carbonates: Evolution of understanding. In: Grotzinger, J., & James, N. (eds.), *Carbonate Sedimentation and Diagenesis in the Evolving Precambrian World*, pp. 320. SEPM Society for Sedimentary Geology.

Halevy, I., Alesker, M., Schuster, E., Popovitz-Biro, R., & Feldman, Y. (2017). A key role for green rust in the Precambrian oceans and the genesis of iron formations. *Nature Geoscience*, *10*, 135–139. https://doi.org/10.1038/ngeo2878

Halevy, I., Peters, S., & Fischer, W. (2012). Sulfate burial constraints on the Phanerozoic sulfur cycle. *Science*, *337*, 331–334. doi:10.1126/science.1220224

Halverson, G., & Hurtgen, M. (2007). Ediacaran growth of the marine sulfate reservoir. *Earth and Planetary Science Letters*, *263*, 32–44. https://doi.org/10.1016/j.epsl.2007.08.022

Hayes, J., Strauss, H., & Kaufman, A. (1999). The abundance of ^{13}C in marine organic matter and isotopic fractionation in the global biogeochemical cycle of carbon during the past 800 Ma. *Chemical Geology*, *161*, 103–125. https://doi.org/10.1016/S0009-2541(99)00083-2

Hayes, J., & Waldbauer, J. (2006). The carbon cycle and associated redox processes through time. *Philosophical Transactions of the Royal Society B*, *361*, 931–950. https://doi.org/10.1098/rstb.2006.1840

Hedges, J., & Keil, R. (1995). Sedimentary organic matter preservation: an assessment and speculative synthesis. *Marine Chemistry*, *49*, 81–115. https://doi.org/10.1016/0304-4203(95)00008-F

Higgins, J., Fischer, W., & Schrag, D. (2009). Oxygenation of the ocean and sediments: Consequences for the seafloor carbonate factory. *Earth and Planetary Science Letters*, *284*, 25–33. https://doi.org/10.1016/j.epsl.2009.03.039

Higgins, J., Blättler, C., Lundstrom, E., Santiago-Ramos, D., Akhtar, A., Crüger Ahm, A., et al. (2018). Mineralogy, early marine diagenesis, and the chemistry of shallow-water carbonate sediments. *Geochimica et Cosmochimica Acta*, *220*, 512–534. https://doi.org/10.1016/j.gca.2017.09.046

Holland, H. (2002). Volcanic gases, black smokers, and the great oxidation event. *Geochimica et Cosmochimica Acta*, *66*, 3811–3826. https://doi.org/10.1016/S0016-7037(02)00950-X

Holser, W., Schidlowski, M., Mackenzie, F., & Maynard, J. (1988). Geochemical cycles of carbon and sulfur. In C. Gregor, R. Garrels, F. Mackenzie, & J. Maynard (eds.), *Chemical Cycles in the Evolution of the Earth*, pp. 105–173. New York: Wiley.

Husson, J., Maloof, A., Schoene, B., Chen, C., & Higgins, J. (2015). Stratigraphic expression of Earth's deepest δ13C excursion in the Wonoka Formation of South Australia. *American Journal of Science*, *315*, 1–45. https://doi.org/10.2475/01.2015.01

Husson, J., & Peters, S. (2017). Atmospheric oxygenation driven by unsteady growth of the continental sedimentary reservoir. *Earth and Planetary Science Letters*, *460*, 68–75. https://doi.org/10.1016/j.epsl.2016.12.012

Katsev, S., & Crowe, S. (2015). Organic carbon burial efficiencies in sediments: The power law of remineralization revisited. *Geology*, *43*, 607–610. https://doi.org/10.1130/G36626.1

Keller, C., Husson, J., Mitchell, R., Bottke, W., Gernon, T., Boehnke, P., et al. (2019). Neoproterozoic glacial origin of the Great Uncomformity. *Proceedings of the National Academy of Sciences of the USA*, *9*, 1136–1145. https://doi.org/10.1073/pnas.1804350116

Key, R., Kozyr, A., Sabine, C., Lee, K., Wanninkhof, R., Bullister, J., et al. (2004). A global ocean carbon climatology: Results from Global Data Analysis Project (GLODAP). *Global Biogeochemical Cycles*, *18*. https://doi.org/10.1029/2004GB002247

Knoll, A., Hayes, J., Kaufman, A., Swett, K., & Lambert, I. (1986). Secular variation in carbon isotope ratios from Upper Proterozoic successions of Svalbard and East Greenland. *Nature*, *321*, 832–838. https://doi.org/10.1038/321832a0

Krause, A., Mills, B., Zhang, S., Planavsky, N., Lenton, T., & Poulton, S. (2018). Stepwise oxygenation of the Paleozoic atmosphere. *Nature Communications*, *9*, 4081. https://doi.org/10.1038/s41467-018-06383-y

Kuntz, L., Laakso, T., Schrag, D., & Crowe, S. (2015). Modeling the carbon cycle in Lake Matano. *Geobiology*, *13*, 454–461. https://doi.org/10.1111/gbi.12141

Laakso, T., & Schrag, D. (2014). Regulation of atmospheric oxygen during the Proterozoic. *Earth and Planetary Science Letters*, *388*, 81–91. https://doi.org/10.1016/j.epsl.2013.11.049

Laakso, T., & Schrag, D. (2017). A theory of atmospheric oxygen. *Geobiology*, *15*, 366–384. https://doi.org/10.1111/gbi.12230

Laakso, T., & Schrag, D. (2018). A small marine biosphere in the Proterozoic. *Geobiology*, *17*, 161–171. https://doi.org/10.1111/gbi.12323

Lee, C., Yeung, L., McKenzie, N., Yokoyama, Y., Ozaki, K., & Lenardic, A. (2016). Two-step rise of atmospheric oxygen linked to the growth of continents. *Nature Geoscience*, *9*, 417–424. https://doi.org/10.1038/ngeo2707

Lenton, T., & Watson, A. (2000). Redfield revisited 2: what regulates the oxygen content of the atmosphere? *Global Biogeochemical Cycles*, *14*, 249–268.

Li, Z., & Lee, C. (2004). The constancy of upper mantle fO_2 through time inferred from V/Sc ratios in basalts. *Earth and Planetary Science Letters*, *228*, 483–493. https://doi.org/10.1016/j.epsl.2004.10.006

Luo, G., Ono, S., Beukes, N., Wang, D., Xie, S., & Summons, R. (2016). Rapid oxygenation of Earth's atmosphere 2.33 billion years ago. *Science Advances*, *2*. doi: 10.1126/sciadv.1600134

Lyons, T., Reinhard, C., & Planavsky, N. (2014). The rise of oxygen in Earth's early ocean and atmosphere. *Nature*, *506*, 307–315. https://doi.org/10.1038/nature13068

Meister, P., McKenzie, J., Vasconcelos, C., Bernasconi, S., Frank, M., Gutjahr, M., & Schrag, D. (2007). Dolomite formation in the dynamic deep biosphere; results from the Peru Margin. *Sedimentology*, *54*, 1007–1032. https://doi.org/10.1111/j.1365-3091.2007.00870.x

Mitnick, E., Lammers, L., Zhang, S., Zaretskiy, Y., & DePaolo, D. (2018). Authigenic carbonate formation rates in marine sediments and implications for the marine $\delta^{13}C$ record. *Earth and Planetary Science Letters*, *495*, 135–145. https://doi.org/10.1016/j.epsl.2018.05.018

Naehr, T., Eichhubl, P., Orphan, V., Hovland, M., Paull, C., Ussler, W., Lorenson, T., & Greene, H. (2007). Authigenic carbonate formation at hydrocarbon seeps in continental margin sediments: a comparative study. *Deep Sea Research II*, *54*, 1268–1291. https://doi.org/10.1016/j.dsr2.2007.04.010

Olson, S., Rehard, C., & Lyons, T. (2016). Limited role for methane in the mid-Proterozoic greenhouse. *Proceedings of the National Academy of Sciences of the USA*, *113*, 11447–11452. https://doi.org/10.1073/pnas.1608549113

Pavlov, A., & Kasting, J. (2002). Mass-independent fractionation of sulfur isotopes in Archean sediments: strong evidence for an anoxic Archean atmosphere. *Astrobiology*, *2*, 27–41. https://doi.org/10.1089/153110702753621321

Planavsky, N., Reinhard, C., Wang, X., Thomson, D., McGoldrick, P., Rainbird, R., Johnson, T., Fischer, W., & Lyons, T. (2014). Low mid-Proterozoic atmospheric oxygen levels and the delayed rise of animals. *Science*, *346*, 635–638. doi:10.1126/science.1258410

Poulton, S., & Canfield, D. (2011). Ferruginous conditions: a dominant feature of the ocean through Earth's history. *Elements*, *7*, 107–112. https://doi.org/10.2113/gselements.7.2.107

Poulton, S., & Raiswell, R. (2004). The low-temperature geochemical cycle of iron: from continental fluxes to marine sediment deposition. *American Journal of Science*, *302*, 774–805. https://doi.org/10.2475/ajs.302.9.774

Prokoph, A., Shields, G., & Veizer, J. (2008). Compilation and time-series analysis of amarine carbonate $\delta^{18}O$, $\delta^{13}C$, $^{87}Sr/^{86}Sr$ and $\delta^{34}S$ database through Earth history. *Earth Science Reviews*, *87*, 113–133. https://doi.org/10.1016/j.earscirev.2007.12.003

Reinhard, C., Planavsky, N., Gill, B., Ozaki, K., Robbins, L., Lyons, T., et al. (2017). Evolution of the global phosphorus cycle. *Nature*, *541*, 386–389. https://doi.org/10.1038/nature20772

Rye, R., & Holland, H. (1998). Paleosols and the evolution of atmospheric oxygen: a critical review. *American Journal of Science*, *298*, 621–672. https://doi.org/10.2475/ajs.298.8.621

Saltzman, M., & Thomas, E. (2012). Carbon isotope stratigraphy. In: F. Gradstein, J. Ogg, M. Schmitz, G. Ogg (eds.), *The Geologic Time Scale 2012*, pp. 207–232. Amsterdam: Elsevier.

Schrag, D., Higgins, J., Macdonald, F., & Johnston, D. (2013). Authigenic carbonate the history of the global carbon cycle. *Science*, *339*, 540–543. doi: 10.1126/science.1229578

Shields, G., & Mills, B. (2017). Tectonic controls on the long-term carbon isotope mass balance. *PNAS*, *114*, 4318–4323. https://doi.org/10.1073/pnas.1614506114

Sleep, N., Meibom, A., Fridriksson, Th., Coleman, R., & Bird, D. (2004). H2-rich fluids from serpentinization: geochemical and biotic implications. *Proceedings of the National Academy of Sciences of the USA*, *101*, 12818–12823. https://doi.org/10.1073/pnas.0405289101

Sperling, E., Frieder, C., Raman, A., Girguis, P., Levin, L., & Knoll, A. (2013). Oxygen, ecology, and the Cambrian radiation of animals. *Proceedings of the National Academy of Sciences of the USA*, *110*, 1244613451. https://doi.org/10.1073/pnas.1312778110

Sperling, E., Wolock, C., Morgan, A., Gill, B., Kunzmann, M., Halverson, G., et al. (2015). Statistical analysis of iron geochemical data suggested limited late Proterozoic oxygenation. *Nature*, *523*, 451–454. https://doi.org/10.1038/nature14589

Sperling, E., & Stockey, R. (2018). The temporal and environmental context of early animal evolution: Considering all the ingredients of an "explosion." *Integrative and Comparative Biology*, *58*, 605–622. https://doi.org/10.1093/icb/icy088

Stolper, D., & Bucholz, C. (2019). Neoproterozoic to early Phanerozoic rise in island arc redox state due to deep ocean oxygenation and increased marine sulfate levels. *Proceedings of the National Academy of Sciences of the USA*, *116*, 8746–8755. https://doi.org/10.1073/pnas.1821847116

Sun, X., & Turchyn, A. (2014). Significant contribution of authigenic carbonate to marine carbon burial. *Nature Geoscience*, *7*, 201–204. https://doi.org/10.1038/ngeo2070

Tostevin, R., Turchyn, A., Farquhar, J., Johnston, D., Eldridge, D., Bishop, J., & McIlvin, M. (2014). Multiple sulfur isotope constraints on the modern sulfur cycle. *Earth and Planetary Science Letters*, *396*, 14–21. https://doi.org/10.1016/j.epsl.2014.03.057

Turcotte, D. (1980). On the thermal evolution of the Earth. *Earth and Planetary Science Letters*, *48*, 5358. https://doi.org/10.1016/0012-821X(80)90169-7

Van Mooy, B., Keil, R., & Devol, A. (2002). Impact of suboxia on sinking particulate organic carbon: Enhanced carbon flux and preferential degradation of amino acids via denitrification. *Geochimica et Cosmochimica Acta*, *66*, 457–465. https://doi.org/10.1016/S0016-7037(01)00787-6

Walker, J., & Brimblecombe, P. (1985). Iron and sulfur in the pre-biologic ocean. *Precambrian Research*, *28*, 205–222. https://doi.org/10.1016/0301-9268(85)90031-2

Walker, J., Hays, P., & Kasting, J. (1981). A negative feedback mechanism for the long-term stabilization of Earth's surface temperature. *Journal of Geophysical Research*, *86*, 9776–9782. https://doi.org/10.1029/JC086iC10p09776

Williams, J., Mills, B., & Lenton, T. (2019). A tectonically driven Ediacaran oxygenation event. *Nature Communications*, *10*, 2690. https://doi.org/10.1038/s41467-019-10286-x

Westrich, J., & Berner, R. (1984). The role of sedimentary organic matter in bacterial sulfate reduction: the G model tested. *Limnology and Oceanography*, *29*, 236–249. https://doi.org/10.4319/lo.1984.29.2.0236